Universidad de Guayaquil

Facultad de Ingeniería Química

INQUIDE
Ingeniería Química y Desarrollo
https://revistas.ug.edu.ec/index.php/iqd

ISSN – p: 1390 –9428 / ISSN – e: 3028-8533 / INQUIDE / Vol. 07 / Nº 01

Thermo-hydraulic design of a helical coil heat exchanger for ethanol cooling

Diseño térmico-hidráulico de un intercambiador de calor de serpentín para el enfriamiento de etanol

Amaury Pérez Sánchez [1] * ; Heily Victoria González [2] ; Arlenis Cristina Alfaro Martínez [3] ; Elizabeth Ranero González [4] ; Eddy Javier Pérez Sánchez [5]

Received: 25/07/2024 – Accepted: 15/11/2024 – Published: 01/01/2025

Research Articles [X] Review Articles [ ] Essay Articles [ ]

* Author for correspondence.

Abstract.
The helical coil configuration is very effective for heat exchangers because they can accommodate a large heat transfer area in a small space, resulting in high heat transfer coefficients. This paper deals with the thermo-hydraulic design of a helical coil heat exchanger to cool an ethanol stream coming from the top of a rectification column, by using a classical, well-known calculation methodology. Several parameters were determined such as the overall heat transfer coefficient (65.88 W/m^2.K); the spiral total surface area (10.75 m^2); the actual number of turns of coil (91) and the height of cylinder (4.12 m). The values of the pressure drop were 290,344 Pa and 0.097 Pa respectively, which are below the limits set by the heat exchange process. The pumping power required for the chilled water (coil-side fluid) stream was 375.21 W, while the pumping power required for the ethanol stream can be considered negligible.

Keywords.
Helical coil heat exchanger, pressure drop, pumping power, spiral surface area, Actual turns of helical coil.

Resumen.
La configuración de serpentín helicoidal es muy efectiva para intercambiadores de calor debido a que pueden acomodar un área de transferencia de calor elevada en un pequeño espacio, resultando en altos coeficientes de transferencia de calor. Este artículo trata acerca del diseño térmico-hidráulico de un intercambiador de calor de serpentín para enfriar una corriente de etanol proveniente del tope de una columna de rectificación, mediante el empleo de una metodología de cálculo clásica bien conocida. Varios parámetros fueron determinados tales como el coeficiente global de transferencia de calor (65,88 W/m2.K), el área superficial total de la espiral (10,75 m2); el número real de vueltas del serpentín (91) y la altura del cilindro (4,12 m). Los valores de la caída de presión fueron de 290 344 Pa y 0,097 Pa, respectivamente, los cuales están por debajo de los límites fijados por el proceso de intercambio de calor. La potencia de bombeo requerida para la corriente de agua fría (fluido que circula por el serpentín) fue de 375,21 W, mientras que la potencia de bombeo requerida para la corriente de etanol puede considerarse despreciable.

Palabras clave.
Intercambiador de calor de serpentín, caída de presión, potencia de bombeo, área superficial de la espiral, vueltas reales del serpentín.

1. Introduction.

Nowadays, due to the increase in energy saving demand in many engineering fields of the modern industry such as heating, ventilation, air conditioning and waste heat recovery, heat exchangers that are more efficient, and have smaller sizes and lower costs are desired, while heat transfer enhancement have been introduced to improve its overall thermo-hydraulic performance [1].

Heat exchangers are widely used in mechanical devices which exchange heat from one type of fluid to another. They are mainly used in heat transfer applications, such as power plants, refrigeration, electronics, air conditioning, chemical and petrochemical processes, automobile devices, and so on [2]. Heat exchangers can improve industrial production efficiency and ensure equipment safety [3], and come in a variety of shapes and sizes, depending on the application: shell and tube, double pipe, spiral or straight, plate type, finned type, helical, among others [2].

Due to their compact structure and high heat transfer coefficient, the helical coil tube heat exchanger (HCHX) has been extensively studied as one of the passive heat transfer enhancements [3].

An HCHX consists of a helical coil fabricated out of a metal pipe that is fitted in the annular portion of two concentric cylinders, as shown in Figure 1. The fluids flow inside the coil and the annulus with heat transfer taking place across the coil wall. The dimensions of both cylinders are determined by the velocity of the fluid in the annulus needed to meet heat-transfer requirements.

[1] University of Camagüey; Faculty of Applied Sciences; amaury.perez84@gmail.com ; https://orcid.org/0000-0002-0819-6760 , Camagüey, Cuba.
[2] University of Camagüey; Faculty of Applied Sciences; heily.victoria@reduc.edu.cu ; https://orcid.org/0009-0007-9319-6506 , Camagüey, Cuba.
[3] Center of Genetic Engineering and Biotechnology of Camagüey; arlenis.alfaro@cigb.edu.cu ; https://orcid.org/0000-0003-2975-6867 , Camagüey, Cuba.
[4] University of Camagüey; Faculty of Applied Sciences; eliza.eddy2202@gmail.com ; https://orcid.org/0000-0001-9755-0276 , Camagüey, Cuba.
[5] Company of Automotive Services S.A.; Commercial Department; eddyjavierpsanchez@gmail.com ; https://orcid.org/0000-0003-4481-1262 , Ciego de Ávila, Cuba.

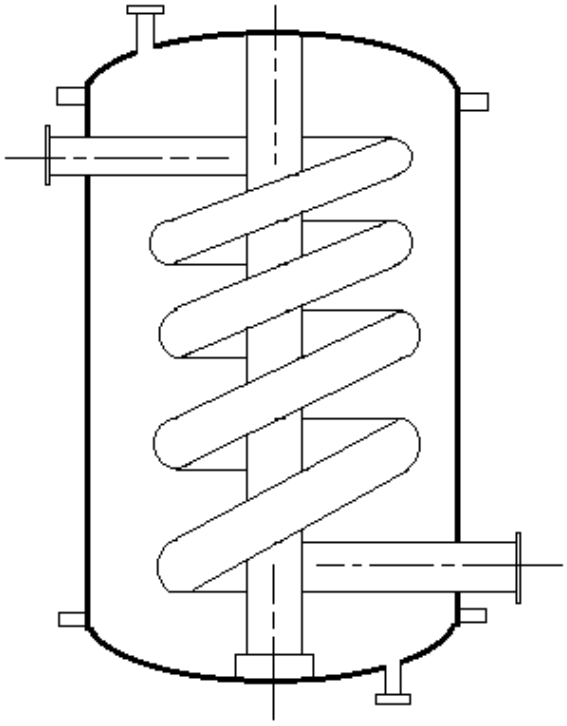

Fig. 1. A helical coil heat exchanger.

Helically coiled exchangers offer certain advantages over the typical heat transfer equipment. Among them it can be mentioned higher film coefficients and heat transfer rate through the tube wall from one fluid to the other, as well as more effective use of available pressure drop, which result in efficient and less-expensive designs. True counter-current flow fully utilizes available logarithmic mean temperature difference, while helical geometry permits handling high temperatures and extreme temperature differentials without highly induced stresses or costly expansion joints. High-pressure capability and the ability to fully clean the service-fluid flow area also add to the exchanger's advantages.

When fluid flows through a helically coiled tube, the curvature of the coil induces centrifugal force [4], which in turn can produce a longitudinal secondary flow in the helically coiled tube, resulting in higher heat transfer efficiency than the value obtained from the straight tubes [3], that is, the centrifugal force induced due to the curvature of the tube results in the secondary flow known as Dean Vortex superimposed on the primary flow which enhances the heat transfer [5]. Fluid flow in a helical tube is characterized by the Dean number, which is a measure of the geometric average of inertial and centrifugal forces to the viscous force ratio, and thus is a measure of a magnitude of the secondary flow [4]. In addition, the coil pitch would influence flow torsion, while depending on the Dean number, the secondary flow pattern within a coiled tube can strongly enhance its heat transfer rate [6].
Helically coiled tubes are useful for various industrial processes such as combustion systems, heat exchangers, solar collectors, and distillation processes because of their simple and effective means of enhancement in heat and mass transfer [7], as well as because they can accommodate a large heat transfer area in compact space, with high heat transfer coefficient [5]. In general they can be used as coolers, heaters, condensers or evaporators [5].

HCHX are broadly used in heating and cooling applications such as heat recovery system, food industries, nuclear power plant, chemical processing, solar water heater, and refrigeration and air-conditioning units because of their simple and effective means of enhancement in heat and mass transfer The HCHX showed increase in the heat transfer rate, effectiveness and overall heat transfer coefficient over the straight tube heat exchanger on all mass flow rates and operating conditions [7].

The merit of the HCHX is that its tube can contact the fluid flowing in the shell side directly, resulting in good heat transfer performance. Therefore, using helical coils in heat exchangers is an effective way for heat transfer enhancement in industries and households [8], although the pressure drop is increased across the heat exchanger, frequently for the coil-side fluid.

In the design of HCHXs, heat transfer performance and pressure loss are significant indicators to consider. It is important to reduce the pressure loss in the helical tube and enhance the heat transfer performance between the shell and tube sides to improve the thermo-hydraulic performance of the helical coil heat exchanger. However, there are many influencing factors on both indices, such as the size of the helical tube, coil pitch, coil diameter, the position of the inlet and outlet streams, and the flow direction, etc. [8]. Heat transfer on HCHX depends largely on the coil size, tube size, mass flow rate, type of thermal fluids and number of turns [7].

Several authors have carried out the design and performance analysis of HCHX. In this sense, [2] numerically investigated the heat transfer performance of a helical heat exchanger using various water-based nanofluids and considering multiple head-ribbed geometries with different coil revolutions. The numerical results were validated against experimental correlations and a published numerical study, thus obtaining as a result that the helical heat exchanger with 2 head ribbed and 30 coil revolutions is the most effective among all the cases and is selected for the nanofluid study. Furthermore, the heat transfer rate could be enhanced by 20%–80% utilizing 2 rib head geometry and by 17%–66% using 30 coil revolutions. Likewise, [8] employed the Computational Fluid Dynamics (CFD) software, ANSYS FLUENT to predict the thermo-hydraulic

performance of an HCHX, including the overall heat transfer coefficient and Fanning friction factor. Using different sizes of the HCHX, comparing the CFD results with experimental data or correlations available in the literature revealed that both results on thermo-hydraulic performance agreed well. Then the Taguchi method was used coupled with grey relational analysis to optimize the HCHX design with the improvement of thermo-hydraulic performance. Among the selected three factors in the optimization process, it was found that the coil pitch and coil diameter were the two most important factors in influencing the thermo-hydraulic performance of HCHXs, while the outer diameter of the helical tube had little impact. Similarly, [1] carried out a three-dimensional study of a shell and helically corrugated coiled tube heat exchanger considering exergy loss, where various design parameters and operating conditions such as corrugation depth, corrugation pitch, the number of rounds, and inlet fluid flow rate on the coil and shell sides, were numerically investigated to examine the heat exchanger hydrothermal performance.

Taguchi analysis was also used to analyze the hydrothermal parameters by considering the interaction effects of them. The results obtained in this study showed that increasing the inlet fluid flow rate on the coil side, corrugation depth and the number of rounds increases both heat transfer and pressure drop, while the most effective parameter that influence on the thermal and hydrodynamic performance of the heat exchanger is the fluid flow rate on the coil side. Also, [3] performed an intelligent optimization scheme on the whole shell and helically coiled tube heat exchanger, where a genetic algorithm was used to automatically determine the coiled pitch, coiled diameter, tube diameter, and flow parameters, in order to maximize the heat transfer rate per thermal surface area by combining the optimization design, structural design, meshing, and numerical calculation. At the same time, the optimization results with and without the pressure drop constraint were compared. The field synergy principle (FSP) was used to explain the cause of the improved performance of the heat exchanger, while the theory of entropy production minimization was employed to evaluate the overall thermal performance. In another study, [5] carried out the analytical and experimental analysis of heat transfer for a finned tube coil heat exchanger immersed in a thermal storage tank, where this tank is equipped with three helical-shaped heating coils and cylindrical-shaped stratification device.

Calculations of thermal power of water coil were made, and correlations of heat transfer coefficients in curved tubes were applied. In order to verify the analytical calculations, the experimental studies of heat transfer characteristic for coil heat exchanger were also performed. Other authors [9] designed HCHX with two different shell configurations, that is, with and without a central core, while both configurations has a copper helical coil. The design was done by using CATIA V5 R2015, and the performance of both the configurations were analyzed and compared by means of Fluid flow (Fluent) in ANSYS for CFD simulations. Saydam [10] designed, fabricated, and experimentally analyzed a prototype phase change material (PCM) heat exchanger with a helical coil tube for its thermal storage performance under different operational conditions. Paraffin wax was used as PCM and an ethylene glycol-water mixture was used as heat transfer fluid (HTF).

Different HTF inlet temperatures, flow directions, and flow rates were tested to find out the effects of these parameters on the performance, including charging and discharging time, of the thermal storage unit. In the work carried out by [11] a supercritical heat exchanger of helical coil type was first designed and then evaluated under real operational conditions. Three heat transfer correlations available from the literature were employed for the design of the heat exchanger. These heat transfer correlations were derived for different working fluids and conditions than the tested organic Rankine cycles. Therefore, to account for the uncertainties of the heat transfer correlations the heat exchanger was oversized by 20%. Finally, performance evaluation of the constructed heat exchanger was performed at supercritical working conditions (laboratory conditions) by examining the influence of several different parameters. [6] proposed a computational fluid dynamics (CFD) methodology to investigate the effects of different Dean (De) number and pitch size on the thermal-hydraulic characteristics in a helically coil-tube heat exchanger with high-temperature helium (He) flowing in the shell side and low-temperature water in the coiled tube.

Three values of De number and four sizes of pitch are considered herein. Based on the simulation results, the complicated phenomena occurred within a helically coiled-tube heat exchanger can be reasonably captured, including the flow acceleration and separation in the shell side, the turbulent wake around the rear of a coiled tube, the secondary flow within the tube, and the developing flow and heat transfer behaviors from the entrance region, etc. [12] performed an experimental investigation of the natural convection heat transfer from helical coiled tubes in water. The outside Nusselt number was correlated to the Rayleigh number using different characteristic lengths, and the relationship obtained was based on a power law equation. The constants in the equation were presented for each of the different characteristic lengths used. The best correlation was using the total height of the coil as the characteristic length.

The developed models were then used to develop a prediction model to predict the outlet temperature of a fluid flowing through a helically coiled heat exchanger, given the inlet temperature, bath temperature, coil dimensions, and fluid flow rate. [13] designed and modeled several unique tube configurations to examine the thermal and hydraulic

Universidad de Guayaquil
Facultad de Ingeniería Química
INQUIDE
Ingeniería Química y Desarrollo
https://revistas.ug.edu.ec/index.php/iqd
ISSN – p: 1390 –9428 / ISSN – e: 3028-8533 / INQUIDE / Vol. 07 / Nº 01

performance of a helical tube heat exchanger both experimentally and numerically. For cold and hot side tube designs, the numerical investigation is completed using three-dimensional modeling, and the findings are confirmed using experimental data with Reynolds numbers ranging from 16,000 to 25,000. The findings showed that, as compared to the uniform tube distribution, the novel tube arrangements have a greater overall heat transfer coefficient, and the performance of heat transfer is dramatically improved, although variations in pressure drop and pumping power are only a little affected.

Other authors presented and successfully implemented a simple mathematical methodology to model the shell and coil heat exchanger [4]; analyzed the performance of a helical coil heat exchanger operating at subcritical and supercritical conditions [14]; introduced an experimental study of horizontal shell and coil heat exchangers in order to determine the effect of coil torsion on heat transfer and pressure drop of shell and coil heat exchangers [15] and determined the convective heat transfer coefficient in both helical and straight tubular heat exchangers under turbulent flow conditions [16].

In certain chemical processing plant it's desired to cool down a stream of ethanol coming from the top of a rectification column, and for that a vertical helical coil heat exchanger was selected as the preferred equipment due to space limitations and the need of achieving a high heat transfer rate. In this context, the present work deals with the design of a helical coil heat exchanger using a well-known, classical calculation methodology, where several parameters are determined such as the actual number of coil turns, calculated spiral total tube length, height of cylinder, spiral total surface area, the pressure drop of both fluids and the pumping power required.

2. Materials and methods.

2.1. Problem definition.

It's desired to cool 750 kg/h of an ethanol stream from 90 ºC to 30 ºC using chilled water at 2 ºC as the cooling medium.
The following data are available for the coil, core tube and shell (Figure 2):

- Shell inner diameter (D_i): 0.46 m.
- Core tube outer diameter (D_K): 0.34 m.
- Average spiral diameter (D_H): 0.40 m.
- Tube outer diameter (d_o): 0.030 m.
- Tube inner diameter (d_i): 0.025 m.

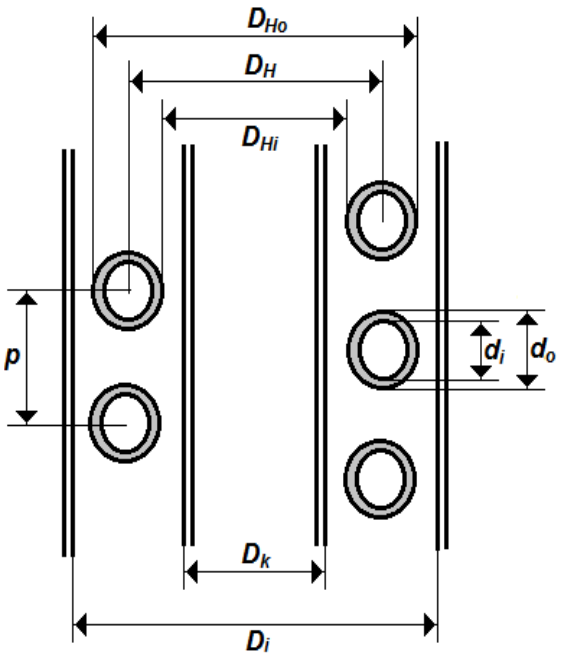

Fig. 2. Geometric parameters of the helical coil heat exchanger.

The outlet temperature of the chilled water should not be higher than 10 ºC, while the fouling factors for the water and ethanol are 0.000176 and 0.000352 K.m^2/W, respectively [17]. The chilled water will be located inside the coil, while the ethanol will flow inside the shell, and both fluids will circulate at countercurrent flow inside the designed helical coil heat exchanger (Figure 2). The coil material is 316 stainless-steel thus having a thermal conductivity of 16.3 W/m.K [18] and the tube pitch, which is the spacing between consecutive coil turns (measured from center to center) (p) can be taken as $1.5 \cdot d_o$. The pressure drop of the shell-side and coil-side fluids must not exceed 0.5 Pa and 300,000 Pa, respectively. Design a suitable helical coil heat exchanger for this heat transfer service.

Universidad de Guayaquil
Facultad de Ingeniería Química
INQUIDE
Ingeniería Química y Desarrollo
https://revistas.ug.edu.ec/index.php/iqd
ISSN – p: 1390 –9428 / ISSN – e: 3028-8533 / INQUIDE / Vol. 07 / Nº 01

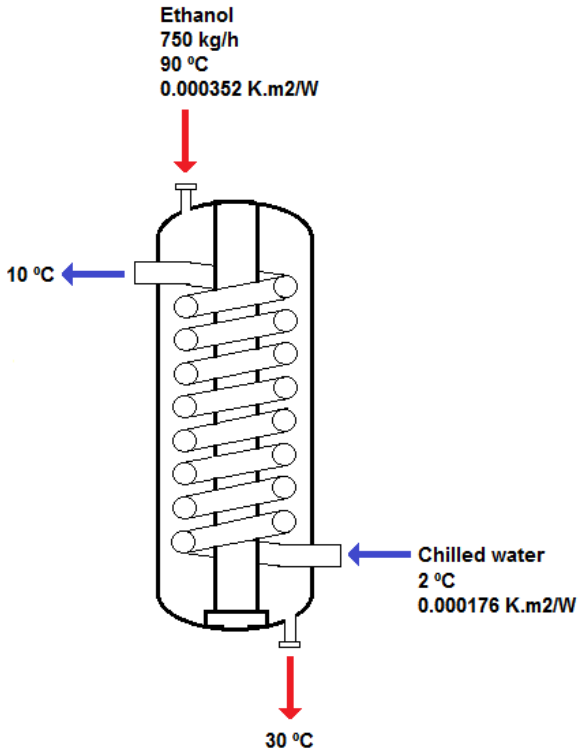

Fig. 3. Schematic view of the proposed helical coil heat exchanger.

2.2. Design methodology.

The equations and correlations reported by [4] [19] [20] were employed to design the helical coil heat exchanger, where several important design parameters are determined such as the overall heat transfer coefficient, the required heat exchange area, the spiral total tube length, the actual number of turns of helical coil, the height of cylinder, as well as the calculated pressure drops and the required pumping power for both fluids.

2.3. Thermal design of the helical coil heat exchanger.

Step 1. Initial data required:

- Mass flowrate of shell-side fluid (m_{shell}).
- Inlet temperature of hot fluid (T_1).
- Outlet temperature of hot fluid (T_2).
- Inlet temperature of cold fluid (t_1).
- Outlet temperature of cold fluid (t_2).
- Fouling factor of hot fluid (R_h).
- Fouling factor of cold fluid (R_c).
- Maximum allowable pressure drop for coil-side fluid ($\Delta P_{coil(A)}$).
- Maximum allowable pressure drop for shell-side fluid ($\Delta P_{shell(A)}$).
- Thermal conductivity of coil material (k_W).
- Shell inner diameter (D_i): 0.46 m.
- Core tube outer diameter (D_K): 0.34 m.
- Average spiral diameter (D_H): 0.40 m.
- Tube outer diameter (d_o): 0.030 m.
- Tube inner diameter (d_i): 0.025 m.
- Tube pitch (p).

Step 2. Average temperature of both fluids:

- Ethanol:

$$\bar{T} = \frac{T_1 + T_2}{2} \quad (1)$$

- Chilled water:

$$\bar{t} = \frac{t_1 + t_2}{2} \quad (2)$$

Step 3. Physical properties of both fluids at the average temperatures determined in the previous step:
The physical properties showed on Table 1 must be determined for both fluids:

Table 1. Physical properties of both fluids.

Physical property	Hot fluid	Cold fluid	Units
Density	ρ_h	ρ_c	kg/m^3
Viscosity	μ_h	μ_c	Pa.s
Heat capacity	Cp_h	Cp_c	kJ/kg.K
Thermal conductivity	k_h	k_c	W/m.K

Source: Own elaboration.

Step 4. Heat load (Q):
Taking the data for the hot fluid (ethanol):

$$Q = \frac{m_{shell} \cdot Cp_h \cdot (T_1 - T_2)}{3{,}600} \quad (3)$$

Step 5. Required mass flowrate of chilled water (m_c):

$$m_{coil} = \frac{Q}{Cp_c \cdot (t_2 - t_1)} \cdot 3{,}600 \quad (4)$$

Step 6. Cross-sectional area of coil (A_{coil}):

ISSN – p: 1390 –9428 / ISSN – e: 3028-8533 / INQUIDE / Vol. 07 / Nº 01

$$A_{coil} = \frac{\pi \cdot d_i^2}{4} \quad (5)$$

Step 7. Volumetric flowrate of coil-side fluid (q_{coil}):

$$q_{coil} = \frac{\frac{m_{coil}}{\rho_c}}{3{,}600} \quad (6)$$

Step 8. Velocity of coil-side fluid (v_{coil}):

$$v_{coil} = \frac{q_{coil}}{A_{coil}} \quad (7)$$

Step 9. Reynolds number of coil-side fluid (Re_{coil}):

$$\mathrm{Re}_{coil} = \frac{d_i \cdot v_{coil} \cdot \rho_c}{\mu_c} \quad (8)$$

Step 10. Prandtl number of the coil-side fluid (Pr_{coil}):

$$\mathrm{Pr}_{coil} = \frac{Cp_c \cdot \mu_c}{k_c} \cdot 1{,}000 \quad (9)$$

Step 11. Nusselt number of the coil-side fluid (Nu_{coil}):

- For $\mathrm{Re}_{coil} > 8{,}000$

$$Nu_{coil} = 0.023 \cdot \mathrm{Re}_{coil}^{0.8} \cdot \mathrm{Pr}_{coil}^{0.33} \quad (10)$$

Step 12. Coil-side heat transfer coefficient (α_{coil}):

$$\alpha_{coil} = \frac{Nu_{coil} \cdot k_c}{d_i} \quad (11)$$

Step 13. Heat transfer coefficient inside coiled tube based on inside diameter [$\alpha_{coil(SP)}$]:

$$\alpha_{coil(SP)} = \alpha_{coil} \cdot \left(1 + 3.5 \cdot \frac{d_i}{D_H}\right) \quad (12)$$

Step 14. Heat transfer coefficient inside coiled tube based on the outside diameter of the coil [$\alpha_{coil(SPa)}$]:

$$\alpha_{coil(SPa)} = \alpha_{coil(SP)} \cdot \frac{d_i}{d_o} \quad (13)$$

Step 15. Outer spiral diameter (D_{Ho}):

$$D_{Ho} = D_i - d_o \quad (14)$$

Step 16. Inner spiral diameter (D_{Hi}):

$$D_{Hi} = D_k + d_o \quad (15)$$

Step 17. Shell-side flow cross-section (A_{shell}):

$$A_{shell} = \frac{\pi}{4} \cdot \left[\left(D_i^2 - D_K^2\right) - \left(D_{Ho}^2 - D_{Hi}^2\right)\right] \quad (16)$$

Step 18. Volumetric flowrate of shell-side fluid (q_{shell}):

$$q_{shell} = \frac{\frac{m_{shell}}{\rho_h}}{3{,}600} \quad (17)$$

Step 19. Flow velocity of the shell-side fluid (v_{shell}):

$$v_{shell} = \frac{q_{shell}}{A_{shell}} \quad (18)$$

Step 20. Reynolds number of shell-side fluid (Re_{shell}):

$$\mathrm{Re}_{shell} = \frac{d_o \cdot v_{shell} \cdot \rho_h}{\mu_h} \quad (19)$$

Step 21. Prandtl number of the shell-side fluid (Pr_{shell}):

$$\mathrm{Pr}_{shell} = \frac{Cp_h \cdot \mu_h}{k_h} \cdot 1{,}000 \quad (20)$$

Step 22. Nusselt number of the shell-side fluid (Nu_{shell}):

$$Nu_{shell} = 0.196 \cdot \mathrm{Re}_{shell}^{0.6} \cdot \mathrm{Pr}_{shell}^{0.33} \quad (21)$$

Step 23. Heat transfer coefficient of shell-side fluid (α_{shell}):

$$\alpha_{shell} = \frac{Nu_{shell} \cdot k_h}{d_o} \quad (22)$$

Step 24. Coil wall thickness (s_W):

$$s_W = \frac{d_0 - d_i}{2} \quad (23)$$

Step 25. Overall heat transfer coefficient (U):

$$U = \frac{1}{\frac{1}{\alpha_{coil(SPa)}} + \frac{1}{\alpha_{shell}} + \frac{s_W}{k_W} + R_h + R_c} \quad (24)$$

Step 26. Logarithmic Mean Temperature Difference ($LMTD$):

- For countercurrent flow:

$$LMTD = \frac{(T_1 - t_2) - (T_2 - t_1)}{\ln \frac{(T_1 - t_2)}{(T_2 - t_1)}} \quad (25)$$

Universidad de Guayaquil
Facultad de Ingeniería Química
INQUIDE
Ingeniería Química y Desarrollo
https://revistas.ug.edu.ec/index.php/iqd
ISSN – p: 1390 –9428 / ISSN – e: 3028-8533 / INQUIDE / Vol. 07 / Nº 01

Step 27. Effective mean temperature difference (ΔT):

$$\Delta T = LMTD \cdot F_t \quad (26)$$

Where F_t is the temperature correction factor = 0.99 [20].

Step 28. Spiral total surface area (A):

$$A = \frac{Q}{U \cdot \Delta T} \cdot 1{,}000 \quad (27)$$

Step 29. Spiral total tube length (L):

$$L = n \cdot \sqrt{(D_H \cdot \pi)^2 + p^2} \quad (28)$$

Step 30. Theoretical number of turns of helical coil (N):

$$N = \frac{A}{\pi \cdot d_o \cdot \frac{L}{n}} \quad (29)$$

Step 31. Actual number of turns of coil (N rounded to the next highest integer) (n):

Step 32. Calculated spiral total tube length (L'):

$$L' = L \cdot n \quad (30)$$

Step 33. Height of cylinder (H):

$$H = n \cdot p + d_o \quad (31)$$

2.4. Pressure drop.

Step 34. Factor E :

$$E = D_H \cdot \left[1 + \left(\frac{p}{\pi \cdot D_H}\right)^2\right] \quad (32)$$

Step 35. Friction factor for flow inside the coil (f):

$$f = \left[\frac{0.3164}{\mathrm{Re}_{coil}^{0.25}} + 0.03 \cdot \left(\frac{d_i}{E}\right)^{1/2}\right] \cdot \left(\frac{\mu_w}{\mu}\right)^{0.27} \quad (33)$$

Where $\left(\mu_w / \mu\right)^{0.27}$ = 1 as suggested by [4]

Step 36. Drag coefficient on coil surface (C_D):

$$C_D = \frac{0.3164}{\mathrm{Re}_{shell}^{0.25}} \cdot \left[1 + 0.095 \cdot \left(\frac{d_o}{D_H}\right)^{1/2} \cdot \mathrm{Re}_{shell}^{0.25}\right] \quad (34)$$

Step 37. Pressure drop for the coil side fluid (ΔP_{coil}):

$$\Delta P_{coil} = f \cdot \frac{L'}{d_i} \cdot \frac{v_{coil}^2 \cdot \rho_c}{2} \quad (35)$$

Step 38. Volume available for the flow of fluid in the annulus (V_{shell}):

$$V_{shell} = \frac{\pi}{4} \cdot \left(D_i^2 - D_K^2\right) \cdot p \cdot n - \frac{\pi}{4} \cdot d_o^2 \cdot L' \quad (36)$$

Step 39. Shell side equivalent diameter (D_e):

$$D_e = \frac{4 \cdot V_{shell}}{\pi \cdot d_o \cdot L'} \quad (37)$$

Step 40. Pressure drop for the shell side fluid (ΔP_{shell}):

$$\Delta P_{shell} = C_D \cdot \frac{H}{D_e} \cdot \frac{v_{shell}^2 \cdot \rho_h}{2} \quad (38)$$

2.5. Pumping power.

Step 41. Pumping power required for the coil side fluid (P_{coil}):

$$P_{coil} = \frac{\Delta P_{coil} \cdot \frac{m_{coil}}{3{,}600}}{\eta_p \cdot \rho_c} \quad (39)$$

Where m_{coil} is given in kg/h and η_p = 0.8 [21].

Step 42. Pumping power required for the shell side fluid (P_{shell}):

$$P_{shell} = \frac{\Delta P_{shell} \cdot \frac{m_{shell}}{3{,}600}}{\eta_p \cdot \rho_h} \quad (40)$$

Where m_{shell} is given in kg/h and η_p = 0.8 [21].

3. Results.

3.1. Design parameters of the helical coil heat exchanger.

Table 2 shows the initial data required to design the helical coil heat exchanger, which are included in Step 1.

Table 2. Initial data required to design the helical coil heat exchanger.

Parameter	Symbol	Value	Unit
Mass flowrate of shell-side fluid	m_{shell}	750	kg/h
Inlet temperature of hot fluid	T_1	90	ºC
Outlet temperature of hot fluid	T_2	30	ºC
Inlet temperature of cold fluid	t_1	2	ºC
Outlet temperature of cold fluid	t_2	10	ºC
Fouling factor of hot fluid	R_h	0.000352	K.m^2/W

ISSN – p: 1390 –9428 / ISSN – e: 3028-8533 / INQUIDE / Vol. 07 / Nº 01

Fouling factor of cold fluid	R_c	0.000176	K.m^2/W
Maximum allowable pressure drop for coil-side fluid	$\Delta P_{coil(A)}$	300,000	Pa
Maximum allowable pressure drop for shell-side fluid	$\Delta P_{shell(A)}$	0.5	Pa
Thermal conductivity of coil material[1]	k_W	16.3	W/m.K
Shell inner diameter	D_i	0.46	m
Core tube outer diameter	D_K	0.34	m
Average spiral diameter	D_H	0.40	m
Tube outer diameter	d_o	0.030	m
Tube inner diameter	d_i	0.025	m
Tube pitch[2]	p	0.045	m

[1]As reported by [22].
[2]Taken as $1.5 \cdot d_o$

Source: Own elaboration.

Step 2. Average temperature of both fluids.

- Ethanol: $\overline{T}$ = 60 ºC
- Chilled wáter: $\bar{t}$ = 6 ºC

Step 3. Physical properties of both fluids at the average temperatures calculated in the previous step.

Table 3 presents the physical properties of both fluids at the average temperatures calculated in the previous step, as reported by [18].

Table 3. Physical property of both fluids.

Physical property	Ethanol	Chilled water	Unit
Density	753.22	999.94	kg/m^3
Viscosity	0.000584	0.001445	Pa.s
Heat capacity	2.781	4.203	kJ/kg.K
Thermal conductivity	0.159	0.572	W/m.K

Source: Own elaboration.

Table 4 exhibits the results of the parameters included in steps 4 to 33.

Table 4. Results of the parameters included in steps 4 to 33.

Step	Parameter	Symbol	Value	Unit
4	Heat load	Q	34.76	kW
5	Required mass flowrate of chilled water	m_{coil}	3,721.63	kg/h
6	Cross-sectional area of coil	A_{coil}	0.00049	m^2
7	Volumetric flowrate of chilled water	q_{coil}	0.0010	m^3/s
8	Velocity of chilled water	v_{coil}	2.04	m/s
9	Reynolds number of chilled water	Re_{coil}	35,292	-
10	Prandtl number of the chilled water	Pr_{coil}	10.62	-
11	Nusselt number of the chilled water[1]	Nu_{coil}	217.93	-
12	Coil-side heat transfer coefficient	α_{coil}	4,986.24	W/m^2.K
13	Heat transfer coefficient inside coiled tube based on inside diameter	$\alpha_{coil(SP)}$	6,076.98	W/m^2.K
14	Heat transfer coefficient inside coiled tube based on the outside diameter of the coil	$\alpha_{coil(SPa)}$	5,064.15	W/m^2.K
15	Outer spiral diameter	D_{Ho}	0.43	m
16	Inner spiral diameter	D_{Hi}	0.37	m
17	Shell-side flow cross-section	A_{shell}	0.0377	m^2
18	Volumetric flowrate of ethanol	q_{shell}	0.0003	m^3/s
19	Flow velocity of the ethanol	v_{shell}	0.008	m/s
20	Reynolds number of ethanol	Re_{shell}	309.54	-

ISSN – p: 1390 –9428 / ISSN – e: 3028-8533 / INQUIDE / Vol. 07 / Nº 01

21	Prandtl number of ethanol	Pr_{shell}	10.21	-
22	Nusselt number of ethanol	Nu_{shell}	13.15	-
23	Heat transfer coefficient of ethanol	α_{shell}	69.70	W/m^2.K
24	Coil wall thickness	s_W	0.0025	m
25	Overall heat transfer coefficient	U	65.88	W/m^2.K
26	Logarithmic Mean Temperature Difference	$LMTD$	49.57	ºC
27	Effective mean temperature difference	ΔT	49.07	ºC
28	Spiral total surface area	A	10.75	m^2
29	Spiral total tube length	L	1.257n	-
30	Theoretical number of turns of helical coil	N	90.78	-
31	Actual number of turns of helical coil	n	91	-
32	Calculated spiral total tube length	L'	114.38	m
33	Height of cylinder	H	4.12	m
34	Factor E	E	0.40	m
35	Friction factor for flow inside the coil	f	0.0305	-
36	Drag coefficient on coil surface	C_D	0.0836	-
37	Pressure drop for the chilled water	ΔP_{coil}	290,344	Pa
38	Volume available for the flow of fluid in the annulus	V_{shell}	0.228	m^3
39	Shell side equivalent diameter	D_e	0.085	m
40	Pressure drop for the ethanol	ΔP_{shell}	0.097	Pa

[1]Equation (10) is valid to use to determine the Nusselt number of chilled water since Re_{coil} > 8,000.
Source: Own elaboration.

3.2. Pressure drop.

Pressure drop increases as fluid flow velocity through the heat exchanger is increased, as does the convection heat transfer coefficient; a good design is therefore always a compromise of sufficiently heat transfer characteristics with acceptable pressure drop.

Table 5 displays the results of the parameters included in steps 34-40, valid to determine the pressure drop of both streams.

Table 5. Results of the parameters calculated in steps 34-40.

Step	Parameter	Symbol	Value	Unit

Source: Own elaboration.

3.3. Pumping power.

Table 6 presents the results of the pumping power required for both fluids.

Table 6. Pumping power required for both fluids.

Step	Parameter	Symbol	Value	Unit
41	Pumping power required for the chilled water	P_{coil}	375.21	W
42	Pumping power required for the ethanol	P_{shell}	0.000034	W

Source: Own elaboration.

4. Discussion.

4.1. Design parameters of the helical coil heat exchanger.

According to the results of Table 4, the heat load had a value of 34.76 kW, while about 3,721.63 kg/h (1.03 kg/s) of chilled water will be necessary to meet the required heat exchange duty. The Reynolds number of chilled water was 35,292, which is 114 times above the Reynolds number of ethanol (309.54). This is due to the relatively high value of the shell-side flow cross-section (0.0377) and the small value of the volumetric flowrate of ethanol (0.0003 m^3/s), which in turn decreases the value of the flow velocity of ethanol (0.008 m/s), thus decreasing the Reynolds number of ethanol (Re_{shell}). The smaller value of the ethanol density (753.22 kg/m^3), as compared to the density of chilled water (999.94 kg/m^3), also affects the small value obtained for Re_{shell}. It's worth stating that the mass flowrate of chilled water is about five times higher than the mass flowrate of ethanol, which therefore influences in the large difference obtained for the Reynolds number of both streams.

ISSN – p: 1390 –9428 / ISSN – e: 3028-8533 / INQUIDE / Vol. 07 / Nº 01

The Nusselt number of the chilled water (217.93) is about 17 times higher than the Nusselt number for ethanol (13.15). This is mainly due to the small value of the Reynolds number obtained for ethanol as compared to the Reynolds number of chilled water. This also influences in that the heat transfer coefficient for the chilled water (5,064.15 W/m^2.K) is about 73 times higher than the heat transfer coefficient for ethanol (69.70 W/m^2.K), although the correlations used to determine these heat transfer coefficients for both fluids are relatively different with each other. Moreover, the values obtained of the Prandtl number for both fluids are almost the same (10.62 for chilled water and 10.21 for ethanol), thus this parameter doesn't affect the calculated values of the heat transfer coefficient for both fluids.

The overall heat transfer coefficient (U) had a value of 65.88 W/m^2.K, which can be classified as low mainly due to the small value obtained of the heat transfer coefficient for the ethanol stream. The rather small value obtained for U influences in the relatively high values obtained for the spiral total surface area (10.75 m^2), the theoretical number of turns of helical coil (90.78) and the height of cylinder (4.12 m). Finally, the calculated spiral total tube length was 114.38 m, while 91 turns of helical coil will be needed for the designed heat exchanger.

In a previous study [23] carried out, a helical coil heat exchanger was designed to cool an acetone stream, where a similar methodology that the one used in this work was applied. In this paper, the acetone mass flowrate is 300 kg/h, while about 1,287 kg/h of chilled water at an inlet temperature of 2 ºC were needed to accomplish the heat transfer duty of cooling the acetone from 70 ºC to 30 ºC. It was obtained a heat transfer coefficient for the chilled water of 1,684.30 kcal/h.m^2.ºC (1,958.84 W/m^2.K) which is about 68 times higher than the heat transfer coefficient for acetone (28.73 W/m^2.K). Also, the Reynolds number of the chilled water (the coil-side fluid) was 11,211, which is 17 times higher than the Reynolds number of acetone (the shell-side fluid). Likewise, the value obtained for the overall heat transfer coefficient was 23.88 kcal/h.m^2.ºC (27.77 W/m^2.K) which can be considered low.

Finally, it was required a heat transfer area of 6.60 m^2, an actual number of turns of helical coil of 53 and a cylinder height of 2.58 m. In general terms, the values of the parameters overall heat transfer coefficient, heat transfer area, actual number of turns of helical coil and cylinder height are higher in the present study as compared to that obtained in [23] due fundamentally to the higher mass flowrate handled for the hot stream. The results found in [23] agree and ratify the results obtained in this study regarding the values of the heat transfer coefficients and the Reynolds numbers for both streams, as well as the validity of the calculated design parameters.

4.2. Pressure drop.

As shown in Table 5, the pressure drop for the coil-side fluid (chilled water) had a value of 290,344 Pa, while the value of this parameter for the shell-side fluid (ethanol) was 0.097 Pa. Both values are below the limits established by the process (300,000 Pa and 0.5 Pa for water and ethanol, respectively). The high value obtained of the pressure drop for the coil-side fluid is due to the small value of the tube inner diameter (0.025 m), as well as the relatively high values of the calculated spiral total tube length (114.38 m), the velocity of chilled water (2.04 m/s) and the density of this fluid (999.94 kg/m^3).

Similarly, the low value of pressure drop obtained for the shell-side fluid is owed mainly to the very low values of the ethanol velocity (0.008 m/s) and the drag coefficient on coil surface (0.0836), as well as to the relatively high value of the shell side equivalent diameter (0.085 m). The same results were obtained in [23], that is, a higher pressure drop was obtained for the coil-side fluid (chilled water: 16,188 Pa) as compared to the pressure drop of the shell-side fluid (acetone: 0.2 Pa). This also agrees with the findings of [4], which reported that the pressure drop at the shell side is significantly smaller than that at the coil side.

Likewise, it can be observed that the higher value obtained for the pressure drop corresponds to the coil-side fluid since it has the highest value of the Reynolds number, which agrees with the reported by [13] and [24]. Also, in [4] it was determined that the pressure drop of both the shell-side and coil-side fluids increase with the increment of the mass flow rate.

4.3. Pumping power.

Regarding the values of Table 6, it will be necessary 375.21 W of pumping power for the chilled water, while the required pumping power for the ethanol can be considered negligible. This is owed mainly to the very small value of the calculated pressure drop obtained for this fluid.

5. Conclusions.

The thermo-hydraulic design of a helical coil heat exchanger was carried out in order to cool an ethanol stream coming from the top of a rectification column and by using a classical, well-known calculation methodology. Several design parameters were determined such as the overall heat transfer coefficient (65.88 W/m^2.K), the spiral total surface area (10.75 m^2), the spiral total tube length (114.38 m), the actual number of turns of helical coil (91) and the height of cylinder (4.12 m). The pressure drop of the coil-side fluid (chilled water) and the shell-side fluid (ethanol) were 290,344 Pa and 0.097 Pa, respectively, which are below the limits established by the heat exchange process for both streams. The pumping power required for the chilled water had a value of 375.21 W, while the pumping power for the ethanol stream can be neglected due to its very low value.

6.- Author Contributions.

1. Conceptualization: Amaury Pérez Sánchez.
2. Data curation: Yerelis Pons García, Elizabeth Ranero González.
3. Formal analysis: Amaury Pérez Sánchez, Daynel Basulto Pita, Eddy Javier Pérez Sánchez.
4. Acquisition of funds: Not applicable.
5. Research: Amaury Pérez Sánchez, Yerelis Pons García, Eddy Javier Pérez Sánchez. 6.
6. Methodology: Amaury Pérez Sánchez, Daynel Basulto Pita, Elizabeth Ranero González.
7. Project administration: Not applicable.
8. Resources: Not applicable.
9. Software: Not applicable.
10. Supervision: Amaury Pérez Sánchez.
11. Validation: Amaury Pérez Sánchez .
12. Writing - original draft: Eddy Javier Pérez Sánchez, Elizabeth Ranero González.
13. Writing - revision and editing: Amaury Pérez Sánchez, Yerelis Pons García.

7.- References.

[1] O. Heydari, M. Miansari, H. Arasteh, and D. Toghraie, "Optimizing the hydrothermal performance of helically corrugated coiled tube heat exchangers using Taguchi's empirical method: energy and exergy analysis," *Journal of Thermal Analysis and Calorimetry*, pp. 1-12, 2020. https://doi.org/10.1007/s10973-020-09808-3

[2] M. J. Hasan, S. F. Ahmed, and A. A. Bhuiyan, "Geometrical and coil revolution effects on the performance enhancement of a helical heat exchanger using nanofluids," *Case Studies in Thermal Engineering*, vol. 35, p. 102106, 2022. https://doi.org/10.1016/j.csite.2022.102106

[3] C. Wang, Z. Cui, H. Yu, K. Chen, and J. Wang, "Intelligent optimization design of shell and helically coiled tube heat exchanger based on genetic algorithm," *International Journal of Heat and Mass Transfer*, vol. 150, p. 120140, 2020. https://doi.org/10.1016/j.ijheatmasstransfer.2020.120140

[4] R. Andrzejczyk and T. Muszynski, "Performance analyses of helical coil heat exchangers. The effect of external coil surface modification on heat exchanger effectiveness," *archives of thermodynamics*, vol. 37, no. 4, pp. 137-159, 2016. https://doi.org/10.1515/aoter-2016-0032

[5] R. Smusz, "Analytical and experimental analysis of tube coil heat exchanger," *Journal of Physics: Conference Series*, vol. 745, p. 032083, 2016. https://doi.org/10.1088/1742-6596/745/3/032083

[6] Y. M. Ferng, W. C. Lin, and C. C. Chieng, "Numerically investigated effects of different Dean number and pitch size on flow and heat transfer characteristics in a helically coil-tube heat exchanger," *Applied Thermal Engineering*, vol. 36, pp. 378-385, 2012. https://doi.org/10.1016/j.applthermaleng.2011.10.052

[7] U. E. Inyang and I. J. Uwa, "Heat Transfer in Helical Coil Heat Exchanger," *Advances in Chemical Engineering and Science*, vol. 12, pp. 26-39, 2022. https://doi.org/10.4236/aces.2022.121003

[8] Y.-C. Shih, Y.-C. Lee, and K.-C. Lin, "Optimized design on the thermohydraulic performance of the helical coil heat exchanger," *International Journal of Thermofluids*, vol. 17, p. 100271, 2023. https://doi.org/10.1016/j.ijft.2022.100271

[9] K. Titus, K. F. Ahmed, S. Kumar, D. Santhosh, and A. V. Geethan, "Design and analysis of helcial coil heat exchanger," *IOP Conf. Series: Materials Science and Engineering*, vol. 923, p. 012016, 2020. https://doi.org/10.1088/1757-899X/923/1/012016

[10] V. Saydam, M. Parsazadeh, M. Radeef, and X. Duan, "Design and experimental analysis of a helical coil phase change heat exchanger for thermal energy storage," *Journal of Energy Storage*, vol. 21, pp. 9-17, 2019. https://doi.org/10.1016/j.est.2018.11.006

[11] M. Lazova, H. Huisseune, A. Kaya, S. Lecompte, G. Kosmadakis, and M. D. Paepe, "Performance Evaluation of a Helical Coil Heat Exchanger Working under Supercritical Conditions in a Solar Organic Rankine Cycle Installation," *Energies*, vol. 9, p. 432, 2016. https://doi.org/10.3390/en9060432

[12] D. G. Prabhanjan, T. J. Rennie, and G. S. V. Raghavan, "Natural convection heat transfer from helical coiled tubes," *International Journal of Thermal Sciences*, vol. 43, pp. 359–365, 2004. https://doi.org/10.1016/j.ijthermalsci.2003.08.005

[13] S. A. Marzouk, M. M. A. Al-Sood, E. M. S. El-Said, M. K. El-Fakharany, and M. M. Younes, "Study of heat transfer and pressure drop for novel configurations of helical tube heat exchanger: a numerical and experimental approach," *Journal of Thermal Analysis and Calorimetry*, pp. 1-16, 2023. https://doi.org/10.1007/s10973-023-12067-7

[14] M. Lazova, A. Kaya, M. Billiet, S. Lecompte, D. Manolakos, and M. D. Paepe, "Experimental Assessment of a Helical Coil Heat Exchanger Operating at Subcritical and Supercritical Conditions in a Small-Scale Solar Organic Rankine Cycle," *Energies*, vol. 10, p. 619, 2017. https://doi.org/10.3390/en10050619

[15] M. R. Salem, K. M. Elshazly, R. Y. Sakr, and R. K. Ali, "Effect of Coil Torsion on Heat Transfer and Pressure Drop Characteristics of Shell and Coil Heat Exchanger," *Journal of Thermal Science and Engineering Applications*, vol. 8, pp. 1-7, 2016. https://doi.org/10.1115/1.4030732

[16] P. Coronel and K. P. Sandeep, "Heat Transfer Coefficient in Helical Heat Exchangers under Turbulent Flow Conditions," *International Journal of Food Engineering*, vol. 4, no. 1, pp. 1-12, 2008. https://doi.org/10.1111/j.1745-4530.2003.tb00602.x

[17] TEMA, *Standards of the Tubular Exchanger Manufacturers Association*, 9th ed. New York, USA: Tubular Exchanger Manufacturers Association, Inc., 2007, p. 298.

[18] D. W. Green and M. Z. Southard, *Perry's Chemical Engineers' Handbook*, 9th ed. New York, USA: McGraw-Hill Education, 2019.

[19] R. K. Patil, B. W. Sende, and P. K. Ghosh, "Designing a helical-coil heat exchanger," *Chemical Engineering*, pp. 85-88, 1982.

[20] M. Nitsche and R. O. Gbadamosi, *Heat Exchanger Design Guide-A Practical Guide for Planning, Selecting and Designing of Shell and Tube Exchangers*. Oxford, UK: Butterworth Heinemann, 2016.

[21] S. Kakaç, H. Liu, and A. Pramuanjaroenkij, *Heat Exchangers - Selection, Rating, and Thermal Design*. Boca Raton, USA: CRC Press, 2012.

[22] R. Sinnott and G. Towler, *Chemical Engineering Design*, 6th ed. Oxford, United Kingdom: Butterworth-Heinemann, 2020.

[23] Pérez, E. J. Pérez, A. Heredia, and L. Pazos, "Diseño de un intercambiador de calor de serpentín para el enfriamiento de acetona," *Nexo*, vol. 32, no. 1, pp. 61-74, 2019. https://doi.org/10.5377/nexo.v32i01.7988

[24] S. A. Nada, W. G. E. Shaer, and A. S. Huzayyin, "Heat transfer and pressure drop characteristics of multi tubes in tube helically coiled heat exchanger," *JP Journal of Heat and Mass Transfer*, vol. 9, no. 2, pp. 173-202, 2014.

Nomenclature.

A	Spiral total surface area	m^2
A_{coil}	Cross-sectional area of coil	m^2
A_{shell}	Shell-side flow cross-section	m^2
C_D	Drag coefficient on coil surface	-
Cp	Heat capacity	kJ/kg.K
d_i	Tube inner diameter	m
d_o	Tube outer diameter	m
D_e	Shell side equivalent diameter	m

ISSN – p: 1390 –9428 / ISSN – e: 3028-8533 / INQUIDE / Vol. 07 / Nº 01

D_H	Average spiral diameter	m
D_{Hi}	Inner spiral diameter	m
D_{Ho}	Outer spiral diameter	m
D_i	Shell inner diameter	m
D_K	Core tube outer diameter	m
E	Factor	m
f	Friction factor for flow inside the coil	-
F_t	Temperature correction factor	-
H	Height of cylinder	m
k	Thermal conductivity	W/m.K
k_W	Thermal conductivity of coil material	W/m.K
L	Spiral total tube length	m
L'	Calculated spiral total tube length	m
$LMTD$	Logarithmic Mean Temperature Difference	°C
m	Mass flowrate	kg/h
n	Actual number of turns of coil	-
N	Theoretical number of turns of helical coil	-
Nu	Nusselt number	-
p	Tube pitch	m
P	Pumping power	W
Pr	Prandtl number	-
ΔP_{coil}	Pressure drop	Pa
$\Delta P_{(A)}$	Maximum allowable pressure drop	Pa
q	Volumetric flowrate	m^3/s
Q	Heat load	kW
R	Fouling factor	$K.m^2/W$
Re	Reynolds number	-
s_W	Coil wall thickness	m
t	Temperature of cold fluid	°C
$\bar{t}$	Average tempereature of cold fluid	°C
T	Temperature of hot fluid	°C
$\bar{T}$	Average temperature of hot fluid	°C
ΔT	Effective mean temperature difference	°C
U	Overall heat transfer coefficient	$W/m^2.K$
v	Velocity	m/s
V_{shell}	Volume available for the flow of fluid in the annulus	m^3

Greek symbols

α	Heat transfer coefficient	$W/m^2.K$
$\alpha_{coil(SP)}$	Heat transfer coefficient inside coiled tube based on inside diameter	$W/m^2.K$
$\alpha_{coil(SPa)}$	Heat transfer coefficient inside coiled tube based on the outside diameter of the coil	$W/m^2.K$
ρ	Density	kg/m^3
μ	Viscosity	Pa.s
η_p	Isentropic efficiency of the pump	-

Subscripts

1	Inlet
2	Outlet
c	Cold
coil	Coil-side fluid
h	Hot
shell	Shell-side fluid